



Synthesis and physicochemical characterization of pigments based on molybdenum « ZnO-MoO₃: Co²⁺ »

H. Lakhlifi¹, M. Benchikhi¹, R. El Ouatib^{1*}, L. Er-Rakho¹,
S. Guillemet-Fritsch² and B. Durand²

¹ Laboratoire de Physico-Chimie des Matériaux Inorganiques, Département de chimie, Faculté des Sciences Ain Chock, Université Hassan II Casablanca, Maroc

² Institut Carnot CIRIMAT, CNRS Université de Toulouse, 118 route de Narbonne, 31062 Toulouse Cedex 9, France.

*Corresponding Author. E-mail: elouatib@yahoo.fr; Tel: (+212661170710)

Abstract

Molybdates Zn_{1-x}Co_xMoO₄ (0 ≤ x ≤ 0.3) were elaborated by the Sol-Gel method with pH=3. The results obtained by DRX show a single-phase domain starting from 500°C for x ≤ 0.3 isostructural to ZnMoO₄. The powder of Zn_{0.7}Co_{0.3}MoO₄ treated at 500°C and 700°C is formed by nano-sized primary crystallites of size between 80 and 160 nm. The colorimetric parameters (L a* b*) of powders obtained at 700°C present a degree of high bluing.

Keywords: Molybdate, Sol-gel, Nanometric, Chromophore, Morphology, Pigment.

Introduction

The molybdates of divalent elements AMoO₄, exhibits numerous structural varieties and especially, polymorphisms with phase transition [1, 2]. These compounds train a big family of oxides being the object of search both in the field of the applied sciences and that of the fundamental sciences. The intrinsically luminescent colorless molybdates, MgMoO₄, ZnMoO₄ and PbMoO₄ [3, 4], are doped with rare earth in order to obtain phosphors [5-7]. Molybdates AMoO₄ with A=Ni²⁺, Co²⁺, Fe²⁺, Mn²⁺, are very studied as catalysts for oxidation of organic compounds [8,9]. Recent studies show that, in tungsten doped copper molybdate CuMo_{1-x}W_xO₄, the temperature of the structural transition α ↔ γ is dependent upon the tungsten content [10,11]. These two polymorphs have different colors, respectively green and brown-red. It is thus possible to envisage the use of this pigment as marker of temperature.

The objective of our work, is to elaborate Zn_{1-x}Co_xMoO₄ pigments. The element cobalt appears to us to be a very promising chromophore for the synthesis of new pigments. The element cobalt appears to us to be a very promising chromophore for the synthesis of new pigments. Indeed, this element is responsible for different tints following the environment which it occupies. In tetrahedral site, it is at the origin of the blue color [11,12]. In octahedral regular site, it is responsible for a pink color [12,13], while a purple tint seems to be obtained when the octahedral site is deformed [10].

The literature also mentions the possibility of the cobalt to take a trigonal bipyramidal based coordination. In molybdate ZnMoO₄, the Zn²⁺ ions are located both in octahedral and in triangular bipyramidal sites [14]. The presence of cobalt in these sites would induce distinguishable colors resulting of the transitions between cobalt d-levels.

Several synthesis methods have been developed to obtain the zinc molybdate, such as the solid method involving solid state reactions between copper and molybdenum oxides. Powders obtained by this method are generally constituted of large-sized particles with low specific surface [15]. The Co-precipitation method has the disadvantage of adsorption at the surface of the particles of foreign ions difficult to remove [16]. To elaborate

our samples of $Zn_{1-x}Co_xMoO_4$ ($x \leq 0.3$), we opted for the polymerizable complex method, that we have already used to prepare the cobalt molybdate [17].

2. Materials and Methods

Commercial reagents used for the synthesis of our compounds are: ammonium heptamolybdate $(NH_4)_6Mo_7O_{24} \cdot 4H_2O$ (Acros, 99%), metal nitrates $((Zn, Co)(NO_3)_2 \cdot 6H_2O)$ (Aldrich, 98%), citric acid (Acros, 98%) and ammonia (NH_4OH) 28% pure, density = 0.91. The aqueous solutions of metals salt 0.2M and ammonium heptamolybdate 0.2M are mixed in stoichiometric proportions. The citric acid is then introduced so that the molar ratio A/M is equal 3 and the pH is fixed to 3. The precursors are obtained after evaporation and drying at $120^\circ C$ for 12 h. These precursors are pre-calcined at $300^\circ C$ for 12 hours under air. The black powders obtained were treated at temperature ranging from 500 to $800^\circ C$. The various steps of this synthesis are given in the **Figure 1**.

The obtained powders were characterized by thermal analysis ATD-ATG (SETARAM TG-DTA 92), by X-rays diffraction (Bruker AXS D4 λ Cu $K\alpha = 1.5418 \text{ \AA}$), by scanning (JEOL-JSM6400) and transmission (JEOL 2010) electronics microscopies. The colorimetric parameters (L a * b *) were measured in the system CIE Lab by means of a colorimeter CR-400 / 410.

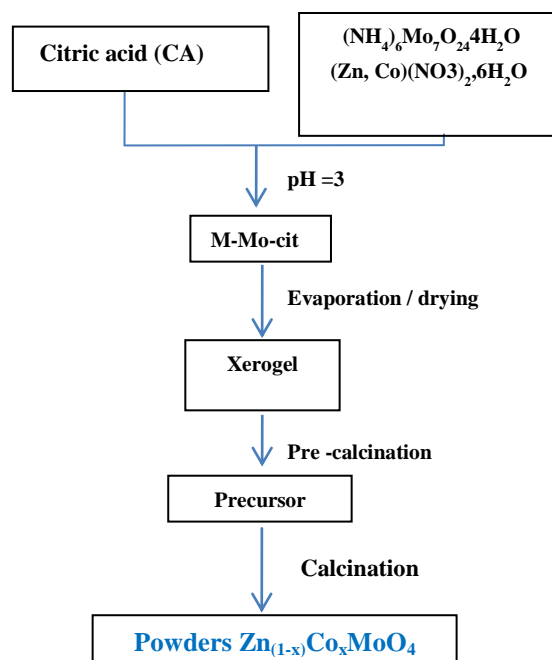


Figure 1: Flowchart of the synthesis of $Zn_{1-x}Co_xMoO_4$ $0 \leq x \leq 0.3$ by the polymerizable complex method

3. Results and discussion

3.1. Structural characterization

The thermally decomposition from precursor $Zn_{0.7}Co_{0.3}MoO_4$ obtained by the drying the gel at $120^\circ C$ was followed by thermal analysis (TGA/DTA). The measures were carried out under air flux at a temperature rate of $2.5^\circ C \text{ min}^{-1}$. Figure 2 shows the typical thermal behavior of the precursor gel. The whole mass loss is about 69%.

The thermogram obtained can be divided into two parts:

- The first weight loss about, 11.5 %, occurring in the range from room temperature to $130^\circ C$, is characterized by an endothermic phenomenon. It is attributed to the dehydration of surface water
- The second weight loss about 57.5 % occurs in the range from $300^\circ C$ to $450^\circ C$. It is characterized by two exothermic peaks, one at $424^\circ C$, attributed to the combustion of organic matter and the other at $460^\circ C$ attributed to the combustion of the residual carbon and crystallization of molybdate. Beyond $500^\circ C$ no loss of mass is observed what indicates that the decomposition is finished.

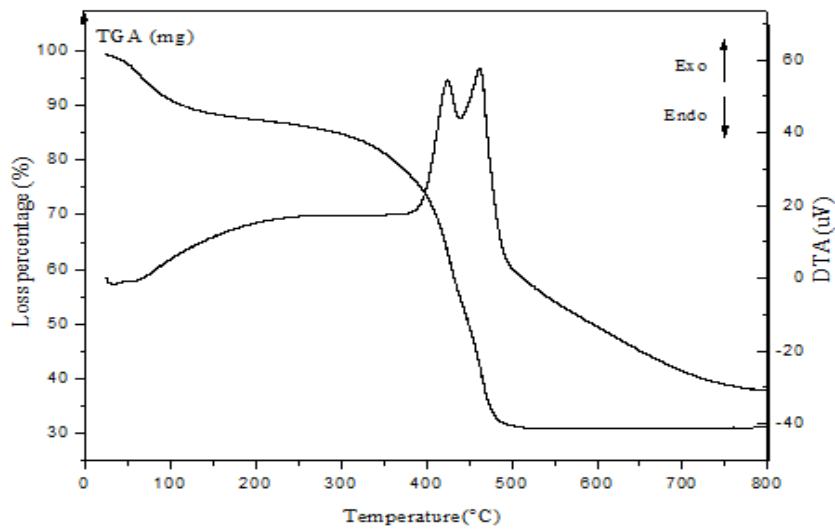


Figure 2: TGA–DTA curves of the $Zn_{0.7}Co_{0.3}MoO_4$ precursor

X-ray diffraction patterns of powders treated at 500 °C for 2 hours are shown in **Figure 3a**. These diagrams show for $x < 0.35$ a mono-phased powder, isostructural with $ZnMoO_4$ (ASTM: 01-070-5387). For $x=0.35$, we note the appearance of an additional phase isostructural with $\beta-CoMoO_4$ (ASTM 00-021-0868). The **Figure 3b** shows the XRD patterns of $Zn_{0.7}Co_{0.3}MoO_4$ treated at temperatures above 500 °C. These diagram shows that this composition is stable above 500°C.

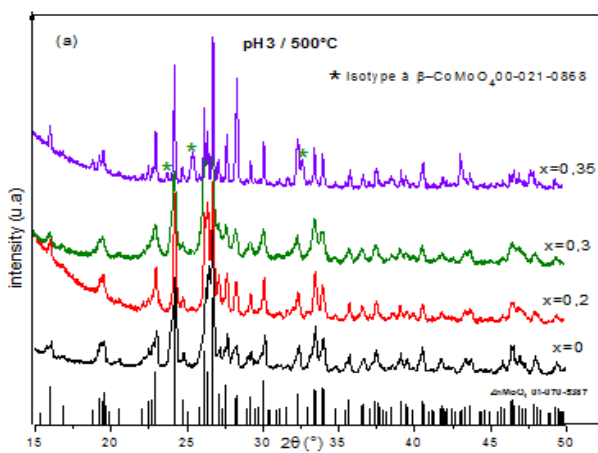


Figure 3a: XRD patterns of $Zn_{1-x}Co_xMoO_4$ ($x \leq 0.35$) treated at 500°C

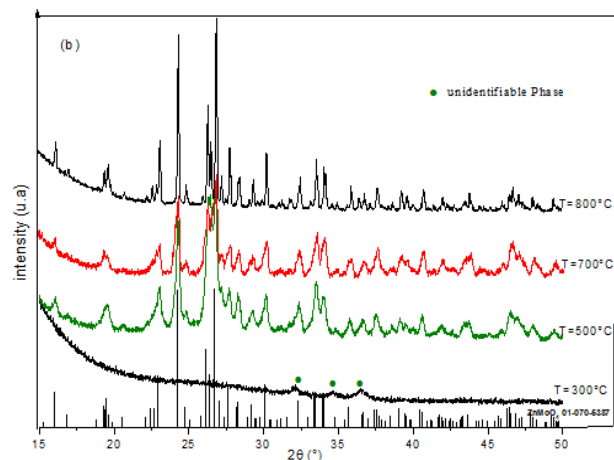


Figure 3b: XRD patterns of $Zn_{0.7}Co_{0.3}MoO_4$ treated at different temperatures

In the rest of the characterization, we considered only the $Zn_{0.7}Co_{0.3}MoO_4$ compound.

3.2. Infrared spectroscopy analysis (FTIR)

The FT-IR spectrum of $Zn_{0.7}Co_{0.3}MoO_4$ precursor powder treated at 500°C during 2 hours **Figure 4** show the presence of the characteristic bands of Mo-O ($749 - 948 \text{ cm}^{-1}$) [18,19] the characteristic strips of vibration of the connection Zn-O ($617-692 \text{ cm}^{-1}$) [20], as well as that of Co-Mo observed at 435 cm^{-1} [21]. These results confirm that the cobalt is successfully incorporated in to the $ZnMoO_4$ crystal structure.

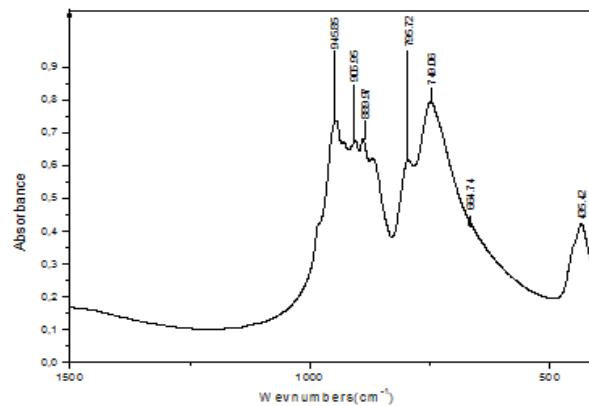


Figure 4: FT-IR spectra of $Zn_{0.7}Co_{0.3}MoO_4$ precursor powders treated at 500°C

3.3. Microstructural characterization

The $Zn_{0.7}Co_{0.3}MoO_4$ powders obtained by calcination for 2h of precursor at 500 , 700 and 800 °C, were examined by scanning (SEM) and transmission (TEM) electron microscopy. The SEM micrographs (Figure 5) show that the powders obtained at 500 and 700°C are formed of agglomerates which size increases with increasing temperature. Examination of the surface of these agglomerates by transmission electron microscopy TEM (Figure 6) shows that these latter are formed of more or less spherical particles of sizes between 80 and 160 nm. These agglomerates become more compact at 800 °C, which shows a certain degree of sintering of the powders at this temperature. According to these results, we note that the best morphology of $Zn_{0.7}Co_{0.3}MoO_4$ is obtained by treatment at 500°C for 2 hours.

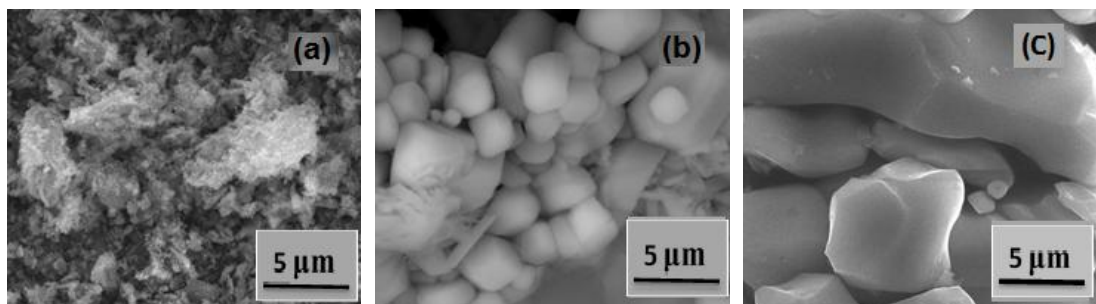


Figure 5: SEM micrograph of $Zn_{0.7}Co_{0.3}MoO_4$ treated at 500° C (a) / 700°C (b) and 800°C (c).

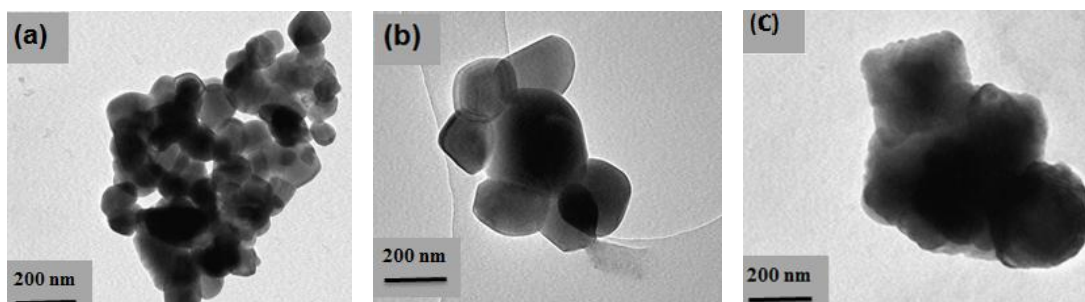


Figure 6: TEM Micrographs of $Zn_{0.7}Co_{0.3}MoO_4$ treated at 500 ° C (a) / 700 ° C (b) and 800 ° C (c).

3.4. Characterization of the color of $Zn_{0.7}Co_{0.3}MoO_4$ powders prepared at 500°C

The variation of the colorimetric parameters (L^* a^* b^*) of $Zn_{0.7}Co_{0.3}MoO_4$ according to the calcination temperature is given in the Figure 7. The evolution of the component ($-b^*$) which characterizes the blue color presents a maximum at 700°C. The component ($-b^*$) coupled with a relatively low value of the red component (a^*) would translate the quality of $Zn_{0.7}Co_{0.3}MoO_4$ with the aim of an application as blue pigment in the ceramic tint.

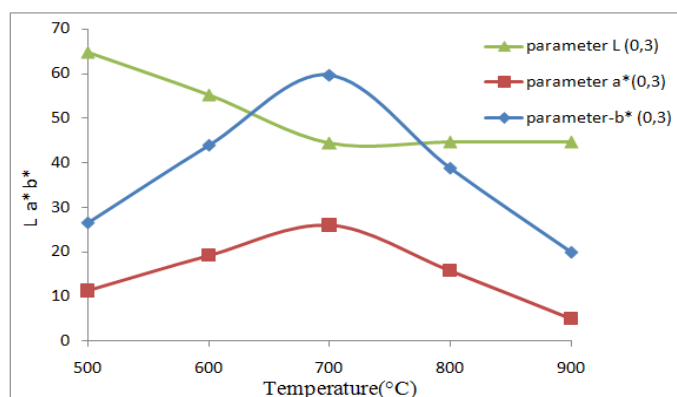


Figure 7: Evolution of the colorimetric parameters of $Zn_{0.7}Co_{0.3}MoO_4$ with the temperature.

Conclusion

During this work, we have been able to develop molybdates $Zn_{1-x}Co_xMoO_4$ ($0 \leq x \leq 0.3$) by sol-gel method at 500°C during 2 hours. The $Zn_{0.7}Co_{0.3}MoO_4$ powders obtained at 500 and at 700°C are formed by grains of size between 80 and 160 nm. The colorimetric parameters (L , a^* , b^*) of this composition shows a high degree of bluing at 700 °C. Polymerizable complex method appears as a simple and reproducible method for preparing $Zn_{1-x}Co_xMoO_4$ based pigments suitable for the coloring of tiles.

References

1. Wang B., Zhou K., Jiang S., Hu Y., and Gui Z., *Poly. Adv. Technol.* 25 (2014) 1419-1425.
2. Matar S.F., Largezeau A., Demazeau G., *Solid State Sci.* 12 (2010), 1779–1785.
3. Mikhailik V. B., Kraus H., Wahl D., Ehrenberg H., Mykhaylyk M.S., *Nucl. Instrum. Methods Phys. Res., Sect. A*, 562 (2006) 513–516.
4. Mikhailik V. B., Kraus H., Itoh M., Iri D. and Uchida M., *J. Phys. Condens. Matter.* 17 (2005) 7209 –7218.
5. Zhou L.Y., Wei J.S., Gong F. Z., Huang J. L., Yi L. H., *J. Solid State Chem.* 181 (2008) 1337-1341.
6. Zhou L.Y., Wei J.S., Gong F. Z., Huang J.L., Yi L. H., Huang, W. Wang, *Mater. Res. Bull.*, 44 (2009) 1411.
7. Junjun Z., Tianqi Z., Lianchun Z., Shucaï G., *J. Photochem. Photobiol., A* 314 (2016) 35–41.
8. Sarkar B., *Heavy Metals In The Environment*, New York, (2002) 446-447.
9. Daturi A M., Savary L., Costentin G., Lavalley J. C., *Catal. Today* 61 (2000) 231–236.
10. Schalkwijk W. A., Scrosati B., *Advances in lithium-ion batteries*, New York, (2002) 121-122.
11. Maoine A., Devillers M., *J. Solid State Chem.* 177 (2004) 2339–2349.
12. Rehren T., *Archaeometry* 43 (2001) 483–489.
13. Wahba A. M., Imam N.G., Mohamed M. B., *J. Mol. Struct.* 1105 (2016) 61-69.
14. Robertson L., Duttine M., Gaudon M., Demourgues A., *Chem. Mater.*, 23 (9) (2011) 2419–2427
DOI: 10.1021/cm200795p.
15. Ehrenberg H., Weitzel H., Paulus H., Wiesmann M., Wltschek G., Geselle M., Fuess H., *J. Phys. Chem. Solids* 58 (1997) 153–160.
16. Fontaine M. L., thesis of Toulouse University III, France (2004).
17. Lakhlifi H., El Ouati R., Er-Rakho L., Durand B., Guillemet-Fritsch S., *MATEC Web of Conferences* 5 (2013) 03001.
18. Bhattacharya S., Kar T., Bar A.K., Roy D., Graca M.P.F., Valente M.A., *Sci. Adv. Mater.* 3 (2011) 284–288.
19. Keereeta Y., Thongtem T., Thongtem S., *Mater. Lett.* 68 (2012) 265–268.
20. Sabet M., Salavati-Niasari M., Davar F., *Mic. Nano Lett.* 6 (2011) 904–908.
21. Kianpour G., Niasari M. S. and Emadi H., *Superlattices Microstruct.* 58 (2013) 120–129.

(2015) ; <http://www.jmaterenvirosci.com>